Early and late cyanobacterial bloomers in a shallow, eutrophic lake

K. J. Painter[1], J. J. Venkiteswaran[2], D. F. Simon[3], S. Vo Duy[3], S. Sauvé[3], and H. M. Baulch[1]

[1] School of Environment and Sustainability, Global Institute for Water Security, University of Saskatchewan, Saskatoon, SK S7N 5C8, Canada

[2] Department of Geography and Environmental Studies, Wilfrid Laurier University, Waterloo,

ON N2L 3C5, Canada

[3] Department of Chemistry, Université de Montréal, Montréal, QC H2V 0B3, Canada

Corresponding author: Kristin Painter (`kristin.painter@usask.ca`)

Key Points:

- We described two key cyanobacterial bloom phases in a critical drinking water supply threatened by blooms of buoyant cyanobacteria

- The mid-summer (early) bloom was dominated by microcystin-producing *Dolichospermum* species

- The autumn (late) *Planktothrix agardhii* bloom was not indicated by chlorophyll-a despite comprising the greatest annual biomass

Abstract

Cyanobacterial blooms present challenges for water treatment, especially in regions like the Canadian prairies where poor water quality intensifies water treatment issues. Buoyant cyanobacteria that resist sedimentation present a challenge as water treatment operators attempt to balance pre-treatment and toxic disinfection by-products. Here, we used microscopy to identify and describe the evolution of cyanobacterial species in Buffalo Pound Lake, a key drinking water supply. We used indicator species analysis to identify temporal grouping structures throughout two sampling seasons from May to October 2018 and 2019. Our findings highlight two key cyanobacterial bloom phases – a mid-summer diazotrophic bloom of *Dolichospermum* spp. and an autumn *Planktothrix agardhii* bloom. *Dolichospermum crassa* and *Woronchinia compacta* served as indicators of the mid-summer and autumn bloom phases, respectively. Different cyanobacterial metabolites were associated with the distinct bloom phases in both years: toxic microcystins were associated with the mid-summer *Dolichospermum* bloom and some newly monitored cyanopeptides (anabaenopeptin A and B) with the autumn *Planktothrix* bloom. Despite forming a significant proportion of the autumn phytoplankton biomass ($> 60\%$), the *Planktothrix* bloom had previously not been detected by sensor or laboratory-derived chlorophyll-*a*. Our results demonstrate the power of targeted taxonomic identification of key species as a tool for managers of bloom-prone systems. Moreover, we describe an autumn *Planktothrix agardhii* bloom that has the potential to disrupt water treatment

due to its evasion of detection. Our findings highlight the importance of identifying this autumn bloom given the expectation that warmer temperatures and a longer ice-free season will become the norm.

1 Introduction

Cyanobacterial bloom frequency and severity is expected to expand globally (Ho et al., 2019; Huisman et al., 2018; Taranu et al., 2015) as the effects of eutrophication (Heisler et al., 2008) and climate change (Kosten et al., 2012; Paerl & Huisman, 2008) become more profound. Especially at risk are the shallow, eutrophic lakes of the North American prairies (Orihel et al., 2012; Schindler & Donahue, 2006). Here, the cumulative impacts of climate change and intensive watershed land use are contributing to increasingly severe cyanobacterial blooms (Binding et al., 2018; Schindler & Donahue, 2006). For example, extensive agriculture and accelerated runoff-driven nutrient transport from land-to-lake have been linked to the rapid eutrophication and subsequent expansion of toxin-producing cyanobacterial blooms in Lake Winnipeg (Ali & English, 2019; Binding et al., 2018; Bunting et al., 2016). Warming surface water temperatures and a longer ice-free season appear to be associated with increasingly potent concentrations of toxic microcystins in shallow, polymictic prairie lakes (Hayes et al., 2020). Moreover, evidence from sediment cores suggests the abundance of toxin-producing cyanobacterial species (e.g., *Dolichospermum* spp.) may be increasing in some prairie lakes (Tse et al., 2018).

Despite these pressures in the Prairies, many waterbodies provide key ecosystem services including critical drinking water supplies. Therefore, understanding algal community composition in bloom-afflicted lakes is critical for effective management. The impacts of cyanobacterial species are of particular concern due to their ability to produce toxic metabolites, thereby presenting potential human health risks. In addition, taste and odour compounds produced by cyanobacteria are costly and difficult to remove from drinking water (Kehoe et al., 2015). The physicochemical properties of many toxin-producing species can also impede their removal during drinking water treatment. For example, filamentous species (e.g., *Aphanizomenon* and *Planktothrix spp.*) can foul filtering infrastructure while others, e.g., *Microcystis* genera, are resistant to coagulation making their removal during sedimentation processes challenging (Jalili et al., 2021; Zamyadi et al., 2019; World Health Organization, 2011). To add to the complexity, Moradinejad et al. (2019) showed that some toxin producing species may persist after oxidation whether they were dominant species or not. Thus, improved understanding of the composition of cyanobacterial blooms and associated toxins is critical to aid in the protection and management of crucial water resources.

High phytoplankton biomass can be particularly difficult to deal with for water treatment operators who must manage particulate loads and balance the use of disinfection processes such as pre-chlorination with the risk of toxic disinfection by-products. When present in large quantities, phytoplankton biomass may contribute to rising floc – aggregates of solid material that cannot be effectively overcome by coagulation (and subsequent sedimentation) alone. Pre-chlorination

(e.g., at the outset of the treatment process prior to clarification and filtering) may reduce problems associated with bloom impacts on processes such as rising flocsby killing buoyant algae (Zamyadi et al. 2021), however, when chlorine reacts with naturally occurring organic matter, toxic trihalomethanes (THMs; chloroform, bromoform, bromodichloromethane, and dibromochloromethane) are produced (Public Health Agency of Canada, 2013). Operators must meet THM limits while maintaining adequate drinking water supplies, thus large accumulations of biomass are potentially problematic.

In addition to the issues associated with biomass accumulation, prairie lakes appear to be especially susceptible to toxin-producing cyanobacterial blooms. For example, Loewen et al. (2021) found a negative correlation between depth and toxin production in Alberta lakes, a link they attributed to the polymictic nature of many shallow prairie lakes whereby frequent mixing provides phosphorus (P) enrichment from deeper waters to phytoplankton. Plentiful P and limited inflow of nitrogen (N) from the watershed throughout the summer months in many prairie systems favours the growth of N-fixing species known to produce toxins (Orihel et al., 2012; Schindler et al., 2012). Shallow prairie lakes are also more susceptible to warming (Gibson et al., 2016), a driver that has also been linked to both blooms (Visser et al., 2016) and toxin production (Hayes et al., 2020). Consequently, improved understanding of the species and associated toxins is needed to guide more in-depth analysis and management of these systems.

Though cyanobacterial blooms are common in shallow prairie lakes, the intra- and interannual variation inherent to the prairie region contributes to the difficulty in predicting the severity of blooms (Vogt et al., 2018) and thus their associated water-treatment issues. As a result, treatment operations may need to be altered quickly in response and the availability of additional tools with high ease-of-use to managers is imperative. In-situ sensors that monitor ambient environmental conditions and non-specific indicators of algal biomass, such as chlorophyll-a (chl-a), have enabled managers to establish links between in-lake algal blooms and water treatment issues (Buffalo Pound Water, 2020; Zamyadi et al., 2016); however, such measurements provide limited information about the organisms responsible for treatment disruptions. Operators of municipal water supplies in Canada also frequently employ routine in-house microscopy to estimate cyanobacterial phytoplankton cell counts as part of source water monitoring (Health Canada, 2021). Thus, additional identification of the presence of key species indicative of cyanobacterial blooms could provide managers with an early indicator of blooms with potential to affect water treatment operations not possible with non-specific biomass indicators.

Here, we examine the structure of the taxonomically identified algal community throughout two ice-free seasons in a shallow polymictic prairie lake that serves as a major drinking water supply. We use a combination of clustering, indicator species analysis, and ordination to describe the succession of algal community abundance over time and identify potential indicator species common across

3

years and time periods. We also provide new information about the types and concentrations of cyanotoxins present and connect toxins to the cyanobacterial community. Finally, we contrast the common algal biomass indicator chl-a and the findings of our taxonomic analysis. The objective of this paper is to identify the seasonal evolution of harmful cyanobacteria and their toxins in a crucial drinking water supply and demonstrate the utility of targeted taxonomic identification of key species as a tool for managers.

2 Materials and Methods

2.1 Site Description

Buffalo Pound Lake is a shallow, polymictic prairie reservoir located in Saskatchewan, Canada (Fig. 1). The lake is approximately 29 km in length, 1.0 km wide and has an average depth of approximately 3.0 m (maximum depth: 5.8 m). Buffalo Pound Lake serves as an important water supply in a relatively water scarce, semi-arid to subhumid region where water quality is affected by eutrophication and annual cyanobacterial blooms (e.g., Schindler & Donahue, 2006; Wheater &Gober, 2013). The lake is an important drinking water source, supplying drinking water to a quarter of the province's population, approximately 260,000 people, in addition to substantive water withdrawals to support industry including local mines. The lake is also used extensively for recreational activities, hosts a provincial park and sport fishery, supports a large provincial fish hatchery, and provides habitat for unique species of special concern, for example the Bigmouth Buffalo, *Ictiobus cyprinellus* (Species At Risk, 2011).

Buffalo Pound Lake is fed primarily by upstream Lake Diefenbaker, a large mesotrophic reservoir, via the Qu'Appelle River. In addition to water from this upstream reservoir, the lake also receives inflow from the local catchment which has a gross drainage area of 3393 km^2 and is predominantly (>70%) agricultural. The effective drainage area (i.e., the area contributing runoff in a median year) is approximately 38% of the gross drainage area (J-M. Davies, Water Security Agency, pers. comm). Local runoff occurs predominantly during the snowmelt period, as is common for most prairie systems (Dumanski et al., 2015). Buffalo Pound Lake's outflow has been controlled since 1939 to regulate water levels for direct and downstream use (Water Security Agency, 2021). Water level is tightly regulated, varying only a few centimeters each year (Terry et al., 2017). Water residence time is short (typically < one year); however, it can vary more than five-fold, depending on precipitation and management decisions (Terry, 2020).
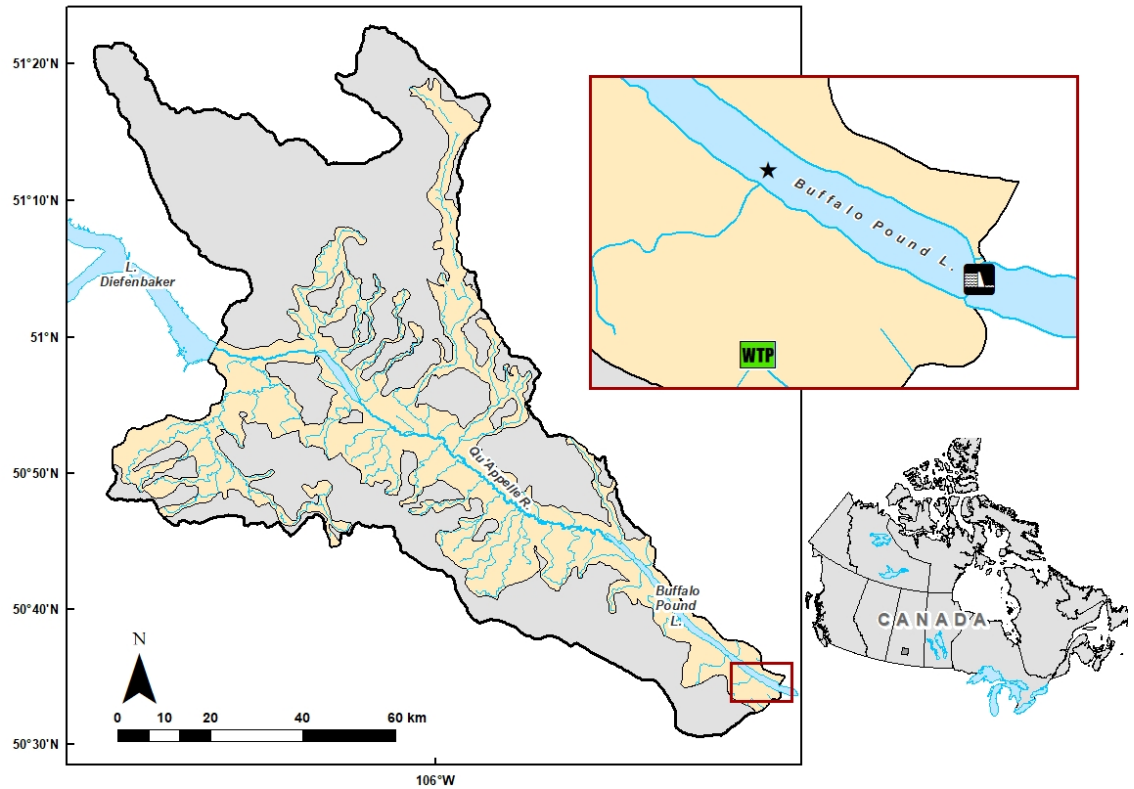
Figure 1. Map of Buffalo Pound Lake, Saskatchewan, Canada, and its gross (grey) and effective (yellow) drainage area, including upstream Lake Diefenbaker. The inset map (red outline) indicates the location of the Buffalo Pound Water Treatment Plant (green WTP symbol) and the sampling site (star symbol; 50°35'8.8" N, 105°23'0.24" W) near its intake. The Buffalo Pound Dam, which controls lake water level, is shown at the southeast end of the lake (black and white dam symbol). Geospatial data used to create this map was downloaded from CanVec (Natural Resources Canada, 2019) and ArcGIS Online (Esri Canada & Nautral Earth Vector, 2020).

Buffalo Pound is a hardwater lake with relatively poor water quality and annual cyanobacterial blooms. The annual range of known concentrations for chl-a is approx. 5.0 to 170 µg/L and < 2.0 to 340 µg/L for total P (Cavaliere & Baulch, 2021). Additionally, dissolved organic matter (DOM) in Buffalo Pound is relatively high for a drinking water source. The poor source water quality creates major challenges for water treatment. One acute example of the challenges managing this water source was seen in 2015 when water shortages occurred resulting from early bloom conditions co-occurring with extreme stratification (CTV News, 2015). Process changes have helped avoid similar incidents, yet problems

remain to manage the concurrent issues of blooms of buoyant cyanobacteria, transient lake stratification, and high DOM.

The drinking water treatment plant uses a process which includes pre-chlorination, coagulation (with alum or polyaluminum chloride), flocculation, clarification, filtration, and then final disinfection before the water is distributed to the cities of Moose Jaw and Regina, Saskatchewan. Cascade degasification and granular activated carbon is used seasonally, near the start and end of the process train respectively while powedered activated carbon is used on an as-needed basis to due reduce excess taste and odour compounds. While pre-chlorination was briefly discontinued to manage disinfection by-products (THMs); issues with flocculation and clarification occurred periodically, associated with bloom periods. These issues have been managed by resuming pre-chlorination, and organic matter concentrations have been lower in recent years (e.g., decline in annual mean dissolved organic C from ~10 mg/L in 2015 to ~5 mg/L in 2020; Buffalo Pound Water, 2020), hence disinfection by-products have remained within regulatory limits. Today, the plant uses in-lake sensor data to help guide short-term adaptation, along with insights from long-term monitoring to guide seasonal changes in processes.

2.2 Sample Collection and Analysis

Water samples were collected periodically during the ice-free season from May to October 2018 and 2019 from a monitoring site located near the Buffalo Pound Water Treatment Plant intake (50°35'8.8" N, 105°23'0.24" W; Fig. 1). On-site water temperature was recorded at 0.2 m depth intervals using a YSI (6500 series) multi-probe sonde (YSI, Ohio, USA; Fig. S1). Discrete grab samples were collected from within the first meter of water at 0.8 m using a Van Dorn sampler and partitioned for phytoplankton enumeration, nutrient chemistry, chl-*a*, and cyanobacterial metabolites. Samples for nutrient chemistry and chl-*a* were collected into acid-washed opaque high density polyethylene bottles and samples for cyanobacterial metabolites were collected into polyethylene terephthalate glycol amber bottles.

Nutrients including soluble reactive P (SRP), ammonium (as $NH_3 + NH_4^+$) and nitrate (as $NO_2^- + NO_3^-$) were analyzed at the Saskatchewan Water Chemistry and Ecology laboratory at the University of Saskatchewan Global Institute for Water Security in Saskatoon, Canada. Samples were filtered through a 0.45 µm nylon syringe-tip filter and frozen until time of analysis. Ammonium samples were preserved additionally with sulfuric acid prior to storage. Samples were analyzed using a SmartChem 170 discrete chemical analyzer (Westco Scientific, USA) using standard EPA methods (SRP, EPA Method PHO-001-A; ammonium, EPA Method AMM-001-A; nitrate, EPA Method NO3-001). Method detection limits were 1.8 g P/L, 5.0 g N/L, and 4.4 g N/L for SRP, ammonium, and nitrate, respectively. Chl-*a* samples were prepared by filtering sample water through glass fiber filters (GF/Fs) and freezing filters until analysis. Prior to analysis, GF/Fs were digested in 95% ethanol for 24 hours (Wintermans & DeMots, 1965) and absorbance of the resulting solution was measured at 649,

6

655 and 750 nm on a Shimadzu UV-1601PC spectrophotometer.

Samples collected for intra- and extracellular cyanobacterial metabolites were filtered through 0.45 µm hydrophilic polypropylene membrane filter. Filters were enclosed in a petri dish and frozen until time of analysis for intracellular metabolites. The resulting filtrate was collected in PETG amber bottles for dissolved (extracellular) toxin analysis and frozen at -20 C until analysis (Dinh et al., 2020). Samples were shipped to Université de Montréal in Montréal, Canada for analysis of total microcystins and 17 cyanobacterial metabolites (see also Texts S1-S2 and Table S1) via on-line solid phase extraction ultra-high performance liquid chromatography coupled to tandem mass spectrometry (Thermo TSQ Quantiva) (Fayad et al., 2015; Munoz et al., 2017) or high-resolution mass spectrometry (Thermo Orbitrap Q-Exactive) (Roy-Lachapelle et al., 2019). Matrix-matched calibration (additions to blank lake water) with internal standard correction was used to quantify cyanotoxins, with accuracies within 81-113% (Roy-Lachapelle et al., 2019).

Phytoplankton samples were preserved with Lugol's iodine upon collection, concentrated, and shipped to Plankton R Us in Winnipeg, Canada for enumeration and identification by D.L. Findlay. Larsen et al. (2020) provide a detailed description of enumeration methods. In brief, samples were enumerated and identified to the species level using an inverted microscope following the methods described in Findlay and Kling (2003). In addition to viable vegetative cells (i.e., with intact chloroplast), cyanobacterial heterocytes were also enumerated if present. Cell counts were converted to wet weight biomass by approximating cell volume using measurements of individual cells and applying the geometric formula best fitted to the shape of the cell per Vollenweider (1968).

2.3 Statistical Analysis

Statistical analyses were conducted using R statistical software (R Core Team, 2021). To better understand patterns in species composition throughout the sampling season, we classified the phytoplankton data from each year into distinct groups. To identify clusters, K-means partitioning was performed on Hellinger standardized (Legendre & Gallagher, 2001) phytoplankton community abundance data (e.g., biomass) with two to five partitions. Then, indicator species analysis was performed on the clustered data sets to identify the ideal number of groupings as described by De Cáceres et al. (2010). The multipatt function in the indicspecies R package (De Cáceres et al., 2020) was used to calculate group-equalized indicator values (IndVals) for each species using untransformed data. IndVals consist of a probability metric and a frequency metric which indicate the likelihood of group membership given detection of the indicator species, and the frequency of species occurrence within a given group, respectively (De Cáceres et al. 2010; Dufrêne & Legendre, 1997). IndVals vary between 0.0 and 1.0, with strength of species association with a particular group increasing from 0.0 (no association) to 1.0 (strong association). A permutation test is used to detect significance of the association between indicators and groups (= 0.05). The number of partitions from two to five

with the highest number of significant indicator species was considered the best grouping.

IndVals were calculated two ways, first considering only the associations between species and each group, and second considering possible associations between species and single groups plus group combinations. Group combinations were included because indicator species associated to two or more groups allow for interpretation of similarity between groupings because they characterize a higher-level grouping structure than would otherwise be indicated by single groups only (De Cáceres et al., 2010).

Prior to analysis of intracellular cyanotoxin data, values below LOD were replaced with zero, and values greater than LOD but less than level of quantification (LOQ) were replaced with their respective LOQs (see Table S1). A squareroot transformation was then applied to the dataset to reduce skewness and the envfit function in R package vegan (Oksanen et al. 2020) was used to fit toxin vectors onto a non-metric multidimensional scaling (NMDS) ordination of the cyanobacterial phytoplankton community using permutation tests. Finally, non-parametric Spearman rank correlations (r_s) were used to assess relationships between the biomass of individual cyanobacterial species and the most predominant toxin concentrations (total microcystins, anabaenopeptins A and B).

3 Results, or a descriptive heading about the results

3.1 Community Composition

The phytoplankton community present in Buffalo Pound Lake consisted of 73 species in the 2018 sampling season and 56 in the 2019 sampling season. In both years, partitioning the community into three groups resulted in the highest number of significant indicator species when only single groups were considered (n = 21 in 2018 and n = 20 in 2019). When group combinations were considered, the highest number of significant indicator species in 2019 was again associated with three groups (n = 19). However, the 2018 data had a higher number of significant indicator species when the community was partitioned into four groups (n = 20) with the second-highest number attributed to three groups (n = 16). However, with four partitions, more than half of the species (11) were associated with a combination grouping of three groups (i.e., species that were present for much of the year) therefore we determined partitioning the 2018 phytoplankton community into three groups to be a more accurate depiction of the change in overall community structure through time.

Despite differences in the overall number of species detected, partitioning placed the phytoplankton community into three similar temporally defined groups in both years: Group A consisting largely of early-season algal species; Group B contained the early to mid-summer blooming diazotrophic cyanophyte species; and Group C was dominated by the late-season non-diazotrophic cyanophyte species (Fig. 2). In 2018 (Fig. 2A), Group A contained only the first two sampling days (late May and early June) and was dominated by chrysophytes (73%

of Group A biomass), especially *Dinobryon sertularia* (43%) and *Chrysochromulina parva* (11%). Cyanophytes accounted for 75% and 70% of 2018 Group B and C biomass, respectively. Group B spanned from mid-June to mid-July (DOY 170 to 193) and also included August 8$^{\text{th}}$ (DOY 220). Three cyanophyte species accounted for much of the biomass: *Dolichospermum flos-aquae* and *D. crassa* accounted for 44% of Group B biomass while *Planktothrix agardhii* contributed 29%. Group C, which included mid-July to mid-September (DOY 197 to 260 but excluding 220), was associated with a shift in the cyanophyte community from *Dolichospermum* spp. dominant to *P. agardhii* dominant. *P. agardhii* contributed 63% of the total biomass in Group C while the *Dolichospermum* species contributed less than 5% collectively.
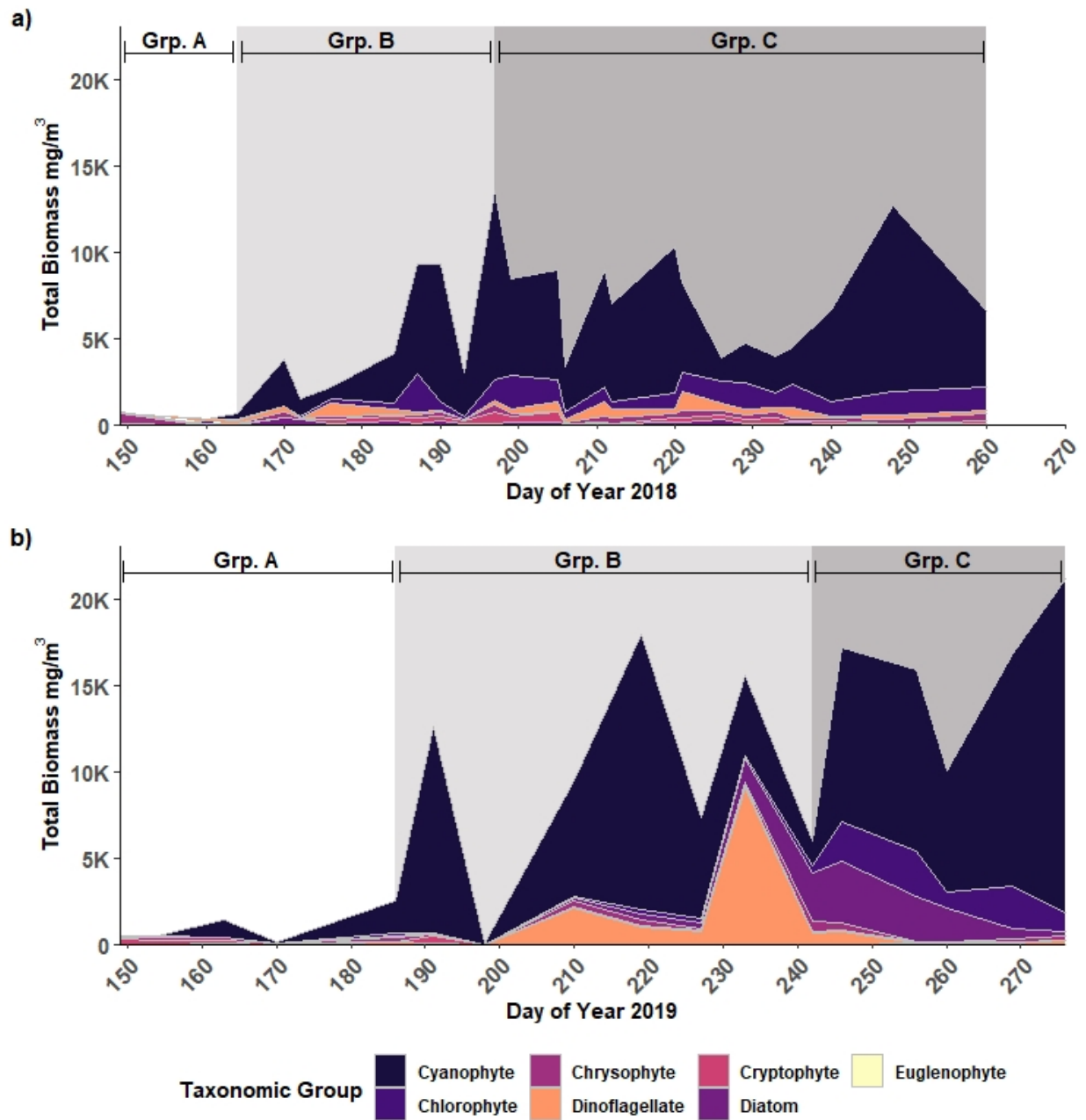
Figure 2. Abundance (measured as biomass in mg/m³) of phytoplankton taxonomic groups from samples collected in a) 2018 and b) 2019 from 0.8 m depth in Buffalo Pound Lake, Saskatchewan. Shading indicates grouping based on K-

means partitioning and indicator species analysis: Group A ("Grp. A"), Group B ("Grp. B"), and Group C ("Grp. C").

In 2019 (Fig. 2B), Group A spanned the first four sampling days, extending later into June (DOY 170) than in 2018. Cryptophytes and chrysophytes accounted for nearly half of the Group A biomass in 2019 (31% and 16% respectively), however, cyanophytes contributed a much larger proportion (43%) than was observed for Group A in 2018 (5%), largely due to *D. flos-aquae* (41% of Group A biomass). Like in 2018, in 2019 cyanophytes accounted for much of the biomass for the remainder of the year: 68% of Group B biomass and 74% of Group C biomass. Group B spanned from early July to late August (DOY 186 to 242) and was again dominated by diazotrophs including *D. crassa* (33%), *D. flos-aquae* (16%) and *Aphanizomenon flos-aquae* (14%). Unlike 2018, *P. agardhii* only accounted for 2% of Group B biomass in 2019; however, it again became the wholly dominant species in Group C (DOY 264 to 276) contributing 63% of the total biomass throughout September.

Individual indicator species were also similar between years. For example, the chrysophyte species *Dinobryon sertularia* was a significant Group A indicator in both 2018 (IndVal = 0.963, p = 0.001) and 2019 (Indval = 1.00, p = 0.001). The diazotrophs *D. crassa* (IndVal = 0.931, p = 0.001) and *A. flos-aquae* (IndVal = 0.997, p = 0.001) were significant indicator species of Group B in 2018 and 2019, respectively. *D. crassa* was an indicator of the combination of Group A and B in 2019 (IndVal = 1.00, p = 0.001). The cyanophyte species *Woronichinia compacta* was a common Group C indicator species in both years (IndVal > 0.960, p = 0.001). Additionally, non-diazotrophic cyanophytes *P. agardhii* (IndVal = 0.990, p = 0.001) and *Merismopedia tenuissima* were Group C indicators (IndVal = 0.834, p = 0.017) in 2019 while *P. agardhii* was an indicator of the Group B and C combination in 2018 (IndVal = 1.00, p = 0.009). A complete list of indicator species by group and group combination and their indicator values can be found in Table S2.

The seasonal patterns apparent in both years indicate a shift from a community dominated by diazotrophic species (i.e., Group B) to non-diazotrophic species (i.e., Group C) composed largely of *Dolichospermum* spp. and *Planktothrix* spp. (Fig. 3A, B; Fig. S2). Nitrogen-fixation during the diazotrophic period was demonstrated by the presence of heterocytes belonging to diazotrophic taxa (*sensu* Boyer 2021) including *D. crassa, D. flos-aquae, and D. solitaria* in 2018 (Fig. 3C) and *D. crassa, D. flos-aquae* and *Aphanizomenon flos-aquae* in 2019 (Fig. 3D). The majority of heterocyte abundance was contributed by *D. crassa* and *D. flos-aquae* (Fig. 3C, D). Both *Dolichospermum* spp. and heterocyte biomass was greater in 2019 (max =11,848 and 942 mg/m^3, respectively) than 2018 (max = 4400 and 357 mg/m^3, respectively), particularly that of *D. crassa*. Nitrogen fixation appeared to be most prevalent during periods of low available N (Fig. 4), for example, the highest ammonium (137 µg/L) and nitrate (44 µg/L) concentrations recorded during our study occurred on DOY 198 in 2019, in the "valley" between the two largest heterocyte biomass peaks (Fig. 3D).
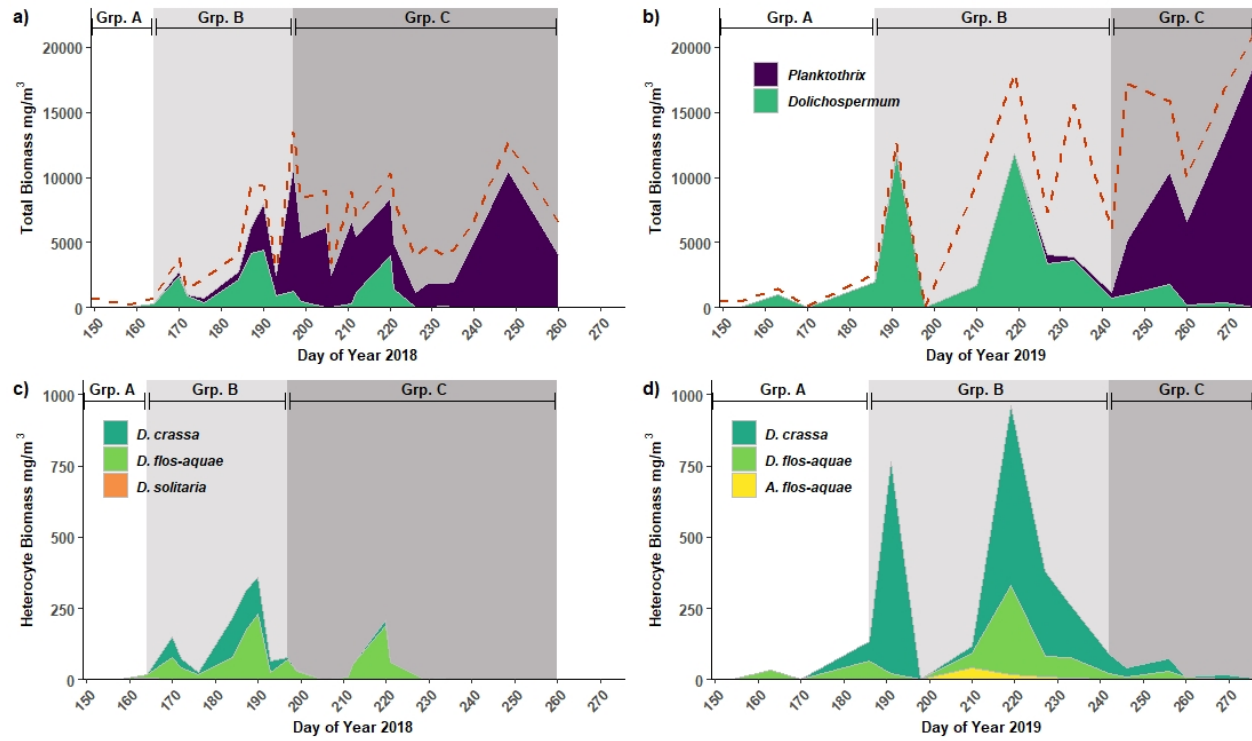
Figure 3. Mid-summer cyanobacterial blooms dominated by nitrogen fixing *Dolichospermum spp.* (green) give way to non-diazotrophic *Planktothirx agardhii* (purple) dominated communities in Buffalo Pound Lake in 2018 (a) and 2019 (b). Dashed line indicates total phytoplankton biomass. Nitrogen fixation is inferred from the presence of heterocytes coinciding with *Dolichospermum spp.* dominated communities in 2018 (c) and 2019 (d). Shading indicates grouping based on K-means partitioning and indicator species analysis: Group A ("Grp. A"), Group B ("Grp. B"), and Group C ("Grp. C").

12
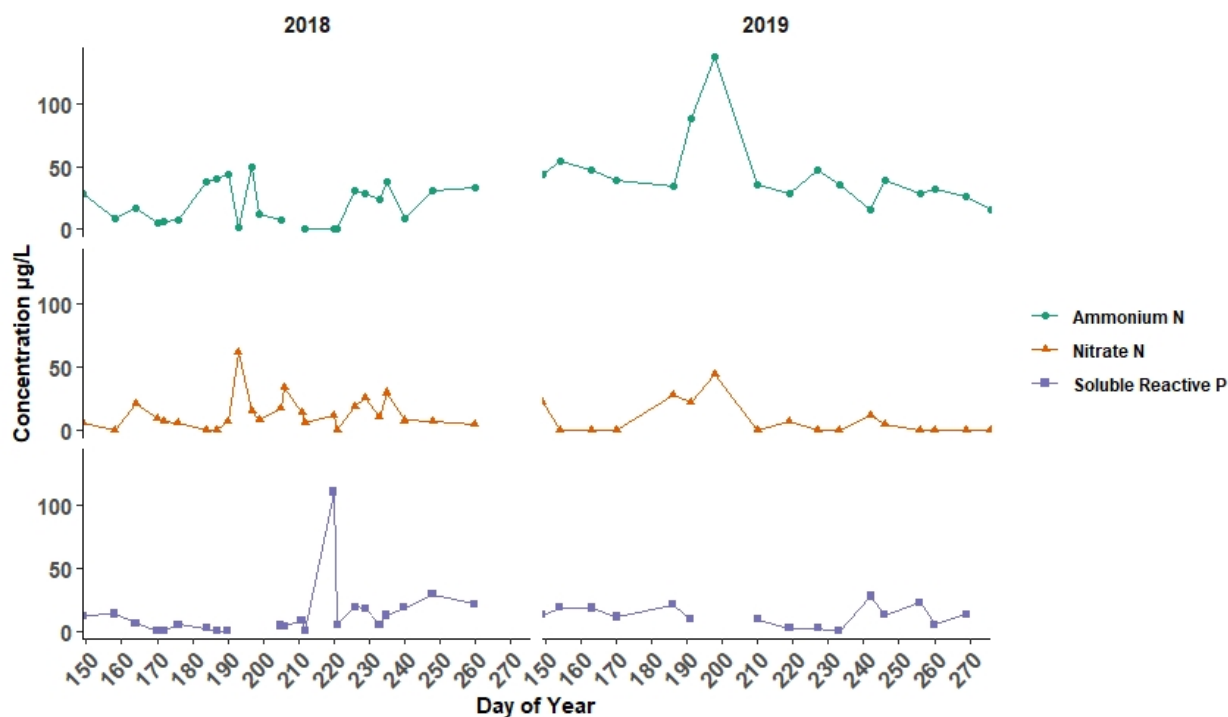
Figure 4. Concentrations of ammonium (as $NH_3 + NH_4^+$; µg N/L), nitrate (as $NO_2^- + NO_3^-$; µg N/L) and soluble reactive phosphorus (µg P/L) in water collected from the 0.8 m depth of Buffalo Pound Lake, Saskatchewan in 2018 and 2019.

3.2 Cyanotoxins

Total microcystins and a suite of 17 cyanometabolites measured in intracellular and extracellular samples in 2018 and 2019 (Table S1; Fig. 5) followed a similar seasonal pattern but differed in concentration. In both years, a seasonal progression was observed from undetectable levels in the early spring to a dominance of microcystin congeners in intracellular samples in the mid-summer coinciding with peak N-fixer biomass (Group B). Microcystins were largely replaced by anabaenopeptins in the late summer and early autumn with peak concentrations occurring at the end of the sampling period coinciding with Group C.
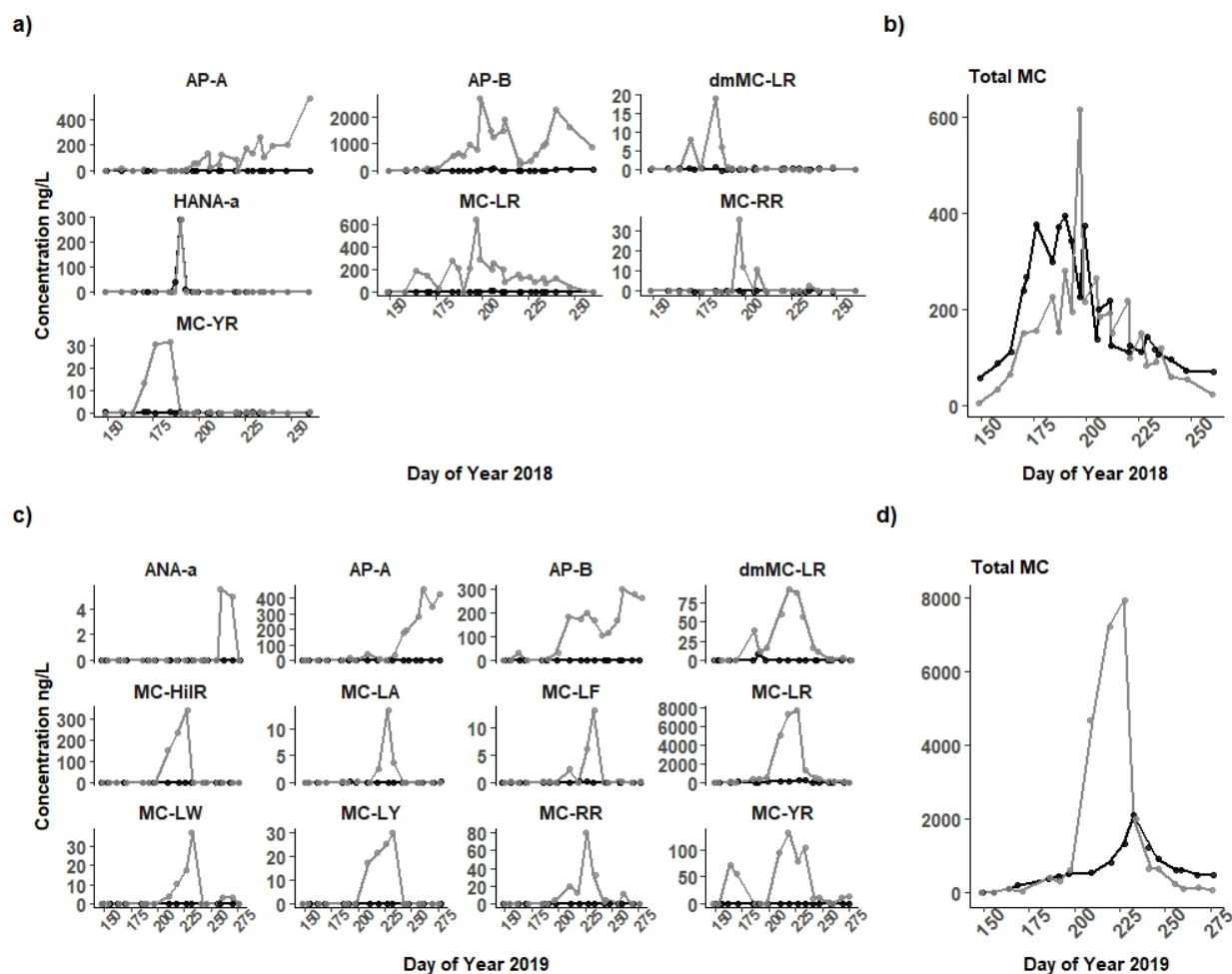
Figure 5. Concentrations (ng/L) of screened intracellular (grey line) and extracellular (black line) cyanobacterial metabolites present in water from the 0.8 m depth of Buffalo Pound Lake in 2018 (a) and 2019 (c) including individual metabolites and total microcystins ("Total MC"; b, d). Only those metabolites that were present above the limit of detection (see Table S1) in each year are shown.

3.2.1 Total Microcystins

The most notable difference in concentrations between years was that of total microcystins. Concentrations of total microcystins were greatest in intracellular samples from Buffalo Pound Lake in both 2018 and 2019; however, concentrations in 2019 were more than an order of magnitude greater (Fig. 5B, D). Total microcystin concentrations in 2018 ranged from < 1.0 to 616 ng/L in intracellular samples and 376 ng/L in extracellular samples. In 2019, intracellular total

14

microcystins ranged from < 10 ng/L in late May and early June to nearly 8000 ng/L in mid-August. Extracellular total microcystins were lower, albeit still much greater than 2018 levels, ranging from < 5.0 to more than 2000 ng/L (on DOY 227) during the same period. These maximum microcystin concentrations are well below the World Health Organization recreational exposure guideline (24 µg/L) and the guideline for short-term exposure (12 µg/L; World Health Organization, 2020). Because total microcystins in extracellular samples were orders of magnitude higher than any individual microcystin congener (see black lines in Fig. 5), it is likely there are unknown microcystins present in Buffalo Pound in addition to the screened common metabolites.

3.2.2 Individual Cyanometabolites

Analysis of individual cyanobacterial metabolites revealed seven individual metabolites present above LOQ in 2018 and 12 individual metabolites present at concentrations above LOQ in 2019 in intracellular samples (Fig. 5A). In 2018, only homo-anatoxin was present in extracellular samples (from DOY 184 to 193, Group A) in addition to total microcystins, reaching a peak concentration of 288 ng/L on DOY 190 in early July. Intracellular toxins present in 2018 included anabaenopeptins A and B, four microcystin congeners (MC-LR, dmMC-LR, MC-RR, and MC-YR), and homo-anatoxin. Microcystins occurred predominately as the congener MC-LR and peaked by mid-July on DOY 197 before falling sharply by half (MC-LR = 293 ng/L on DOY 199). Anabaenopeptin B concentrations increased gradually from ~100 ng/L in late June to ~1000 ng/L in mid-July on DOY 197, and then more than doubled between DOY 197 and 199, reaching 2706 ng/L on DOY 199 immediately following the drop in microcystin concentration. Anabaenopeptin B fell to 228 ng/L by mid-August (DOY 221) but peaked a second time (2296 ng/L) on DOY 240. Anabaenopeptin A also began to increase after microcystins declined with the highest concentration (570 ng/L) observed on the last day of sampling in September (DOY 260).

Of the 12 individual metabolites present in 2019 intracellular samples, nine were microcystin congeners (MC-LR, dmMC-LR, MC-HiIR, MC-LA, MC-LF, MC-LW, MC-LY, MC-RR, and MC-YR), and the remainder included anabaenopeptin A and B, and anatoxin-A (Fig. 5C). Only MC-LR and dmMC-LR were present in extracellular samples, both below 50 ng/L. As in 2018, the most prevalent microcystin congener in intracellular samples was MC-LR (from < 10 to 7664 ng/L); MC-LR and the other microcystin congeners present peaked in mid-August (DOY 227), approximately one month later than in 2018 but again corresponding with Group B. Anatoxin-A was present in very small concentrations (below its LOQ, max = 6 ng/L) in September. Both anabaenopeptin A and B (max = 459 and 303 ng/L, respectively) peaked in September on DOY 260. Like in 2018, anabaenopeptin B concentrations also appeared to peak twice, the first smaller peak (202 ng/L) co-occurring with the microcystin peak and the second (303 ng/L) occurring on DOY 260. However, anabaenopeptin B was present at far lower concentrations in 2019 than in the

previous year.

3.2.2 Co-occurrence of cyanotoxins and cyanobacterial species

The changing concentration and composition of intracellular cyanotoxins throughout the 2018 and 2019 sampling seasons co-occurred with changing cyanobacterial phytoplankton community composition as indicated by non-metric multidimensional scaling (NMDS) ordinations (2018 stress = 0.091; 2019 stress = 0.072; Fig. 6). Vectors, representing intracellular toxins and total microcystins, fit on to the ordinations point to distinct groups of species associated with microcystins and anabaenopeptins. Moreover, the composition of these groups was similar between years.
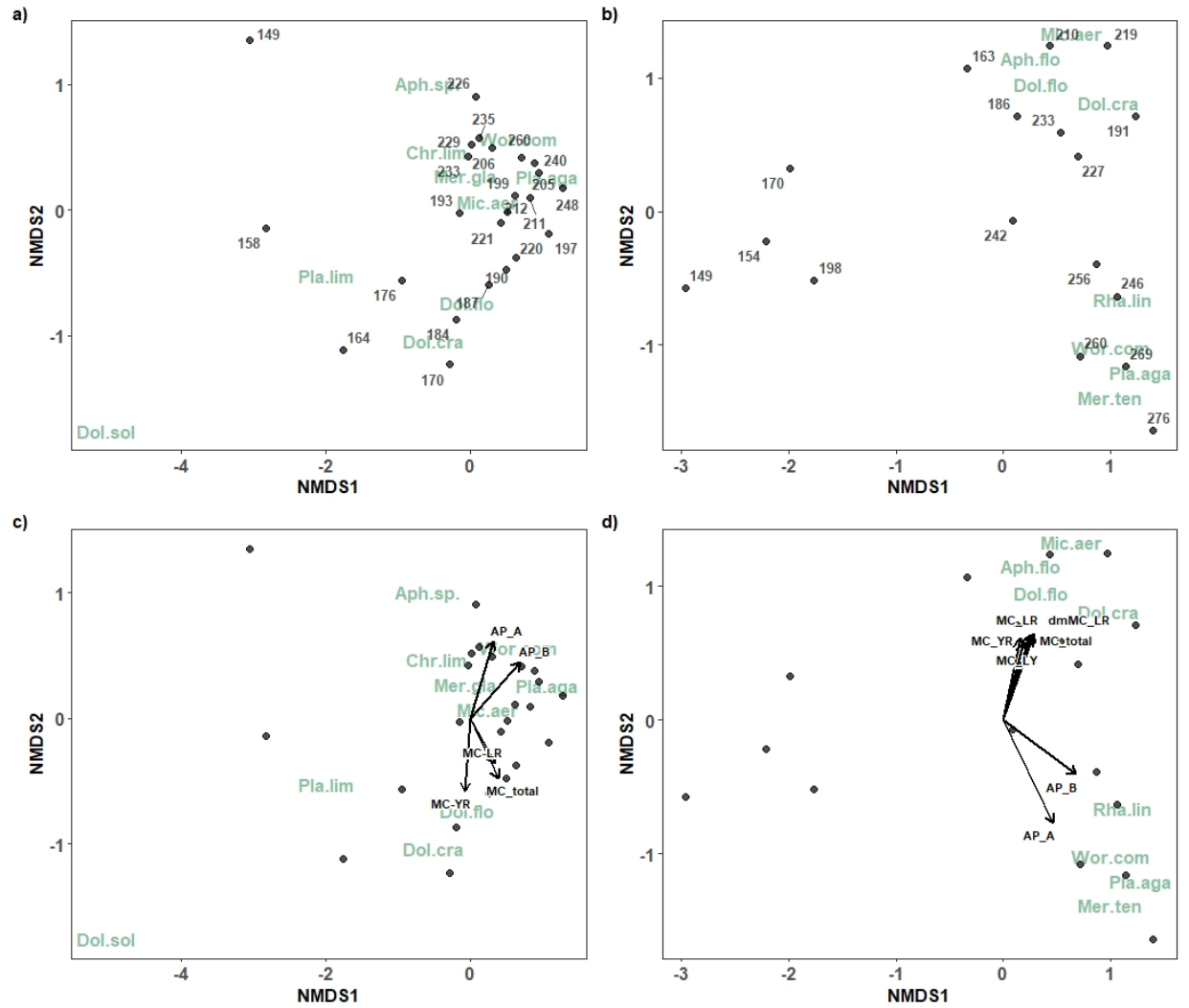
Figure 6. Non-metric multidimensional scaling plots of cyanobacterial phytoplankton community composition throughout the 2018 (stress = 0.091; a, c) and 2019 (stress = 0.072; b, d) sampling seasons. Points indicate day of year in 2018 (a, c) and 2019 (b, d). Abbreviated species name codes using the first three letters of genus and species (gen.spe; shown in green) represent cyanobacterial species. Vectors represent toxins (see Table S1 for abbreviations) for which permutation tests were significant (p > 0.05) in 2018 (c) and 2019 (d) with vector length indicating strength of correlation.

For example, in 2018, significant vectors showed an association between (total microcystins ($r^2 = 0.39$, p = 0.005) and several microcystin congeners (dmMC-LR, $r^2 = 0.30$, p = 0.035; and MC-YR, $r^2 = 0.35$, p = 0.016) and the Group B (DOYs 184 to 212) cyanobacterial community dominated by diazotrophic taxa (e.g., *D. crassa and D. flos-aquae)*. The strongest associations were those between anabaenopeptin A ($r^2 = 0.48$, p = 0.002) and anabaenopeptin B ($r^2 = 0.68$, p = 0.001) and the late-season Group C (e.g., DOYs 235 to 260) cyanobacterial community dominated by *Planktothrix agardhii.*

Similarly, in 2019, microcystins were also correlated with the mid-season (DOYs 186 to 227, or Group B) bloom comprised largely of the N-fixing taxa (*Dolichospermum flos-aquae*, *D. crassa, A. flos-aquae*) and which also included *Microcystis aeruginosa.* Total microcystins ($r^2 = 0.45$, p = 0.014) and four microcystin congeners, MC-LR ($r^2 = 0.47$, p = 0.01), dmMC-LR ($r^2 = 0.49$, p = 0.008), MC-LY ($r^2 = 0.37$, p = 0.039), and MC-YR ($r^2 = 0.39$, p = 0.036) were significantly correlated to the mid-season bloom cyanobacterial community. Anabaenopeptins A ($r^2 = 0.81$, p = 0.001) and B ($r^2 = 0.63$, p = 0.001) were most strongly correlated with the cyanobacterial community present after DOY 246 (Group C) which was largely dominated by *P. agardhii,* but also included *Woronichinia compacta*, *Rhabdogloea linearis*, and *Merismopedia tenuissima.*

Spearman rank correlations between the biomass of individual cyanobacterial species and the most prevalent intracellular cyanotoxins (total microcystins, anabaenopeptins A and B) in 2018 and 2019 were again suggestive of links between the Group B species and microcystins, and non-diazotrophic Group C species and anabaenopeptins. In 2018, correlations were strongest between total microcystins and diazotrophic *D. crassa* ($r_s = 0.68$, p <0.001) as well as *D. flos-aquae* ($r_s = 0.57$, p = 0.003) and non-diazotrophic *M. aeruginosa (*$r_s = 0.52$, p = 0.009). Anabaenopeptin A was most strongly correlated with *W. compacta* biomass ($r_s = 0.78$, p < 0.001) and *P. agardhii* ($r_s = 0.49$, p = 0.01) but also negatively correlated with *D. crassa* ($r_s = -0.53$, p = 0.007) and *D. flos-aquae* ($r_s = -0.49$, p = 0.02). Anabaenopeptin B was most strongly correlated with *P. agardhii* ($r_s = 0.76$, p < 0.001) and *W. compacta* ($r_s = 0.57$, p = 0.003).

Of the Spearman rank correlations between the biomass of cyanobacterial species present in 2019 and intracellular toxins, the strongest was between total microcystins and *A. flos-aquae* ($r_s = 0.92$, p < 0.001). Significant positive correlations also existed between total microcystins and *D. crassa* ($r_s = 0.74$, p = 0.001), *D. flos-aquae* ($r_s = 0.72$, p = 0.001), *M. aeruginosa* ($r_s = 0.69$, p

= 0.002), and *R. lineare* (r_s = 0.56, p = 0.02). Anabaenopeptin A was most strongly correlated with *P. agardhii* (r_s = 0.77, p <0.001) and *W. compacta* biomass (r_s = 0.78, p < 0.001) as well as *M. teniuissima* (r_s = 0.67, p = 0.002). Anabaenopeptin B was correlated with the same species (*P. agardhii*, r_s = 0.65, p = 0.004; *W. compacta*, r_s = 0.64, p = 0.006; *M. teniussima*, r_s = 0.61, p =0.008) although these correlations were slightly weaker.

When the results of the Spearman rank correlations are taken into consideration alongside the results of the indicator species analysis, some key similarities are apparent. For example, *D. crassa* was an indicator for Group B in 2018, and the combination Group B + C in 2019, and *A. flos-aquae* was an indicator of Group B in 2018. Both species were strongly correlated with microcystins suggesting that they serve as important indicators of potentially toxic mid-summer bloom formation. *W. compacta* was an indicator of Group C in both years and correlated with the anabaenopeptins. Its presence appears to indicate a shift from a primarily microcystin-producing N-fixing bloom to an anabaenopeptin-producing bloom comprised largely of filamentous *Planktothrix.*

3.3 Comparison of taxonomy and chlorophyll-*a*

The period when *Planktothrix* dominated the community leading to high biomass was not accompanied by a similar peak in chl-*a*, suggesting it is not well indicated by chl-*a* (Fig. 7). In both years, when *Planktothrix agardhii* biomass was greatest in September (Fig. 7A), chl-*a* concentrations measured from the same parcel of water from which taxonomy samples were collected were relatively low (Fig. 7B). For example, in 2018, the highest chl-*a* concentration (92 µg/L) occurred in early July (DOY 190), while peak Planktothrix biomass (> 10,000 mg/m^3) and near peak total biomass (>12, 500 mg/m^3) occurred in early September (DOY 248) when chl-*a* was only 20 µg/L. Similarly, in 2019 chl-*a* reached peak concentration (118 µg/L) in early August (DOY 219) but had dropped to 29 µg/L when *Planktothrix* (> 18,500 mg/m^3) and total biomass (> 21,000 mg/m^3) were at their peak on DOY 260 in mid-September.
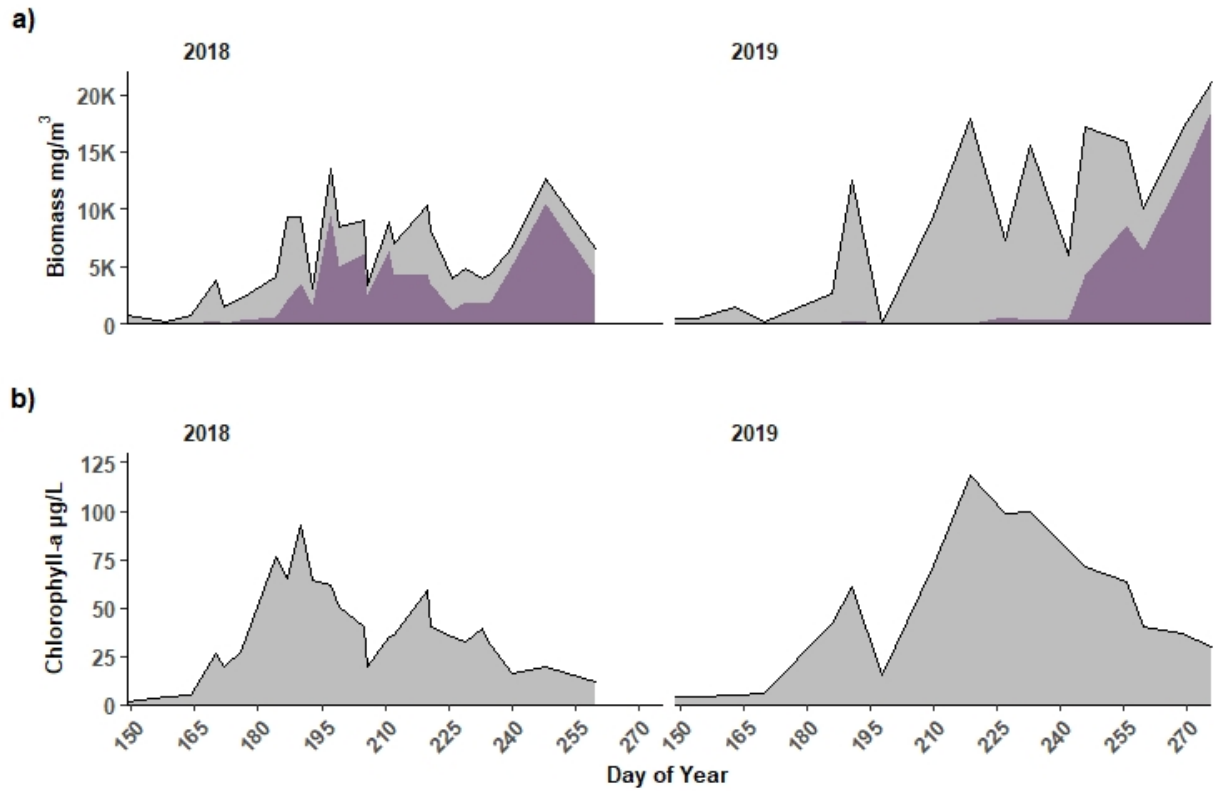
Figure 7. a) Total phytoplankton biomass (grey shaded area) including Planktothrix agardhii biomass (darker purple shading) and b) chlorophyll-a concentration measured in samples collected from 0.8m depth in Buffalo Pound Lake, Saskatchewan in 2018 and 2019.

4 Discussion

Cyanobacterial blooms in drinking water sources, such as Buffalo Pound Lake, can increase risks to water treatment operations. Consequently, managers are required to carefully monitor bloom-impacted systems to ensure treatment processes remain unaffected by cyanobacteria. Here we have demonstrated the progression of cyanobacteria-dominated blooms from diazotrophs to *Planktothrix agardhii* in a critical drinking water supply and have identified the potential for each bloom phase to produce suites of cyanotoxins. Moreover, we discerned that key indicator phytoplankton species can be valuable monitoring tools to help anticipate the timing, magnitude, and toxin dynamics of cyanobacterial bloom phases.

Our results showed that phytoplankton community structure in Buffalo Pound Lake changed seasonally but did so in a consistent pattern. Cryptophytes and

19

chrysophtes (i.e., Group A) were succeeded by N-fixing cyanobacteria, especially *Dolichospermum* spp. (i.e., Group B). By September much of the community was composed of non-diazotrophic *Planktothrix agardhii* (i.e., Group C). Though this general pattern was consistent between years, the timing of succession between groups differed as did their abundance. Despite these differences, we were able to identify indicators of the successional groups that were, for the most part, common across years.

The succession from non-cyanobacterial species to a diazotroph-dominated community in the warm summer months is well established for temperate eutrophic lakes (e.g., Orihel et al., 2015; Persaud et al., 2015). In the prairie region, diazotrophic blooms have received much research attention by limnologists (e.g., Bogard et al., 2020; Bunting et al., 2016; Hayes et al., 2019) given highly productive prairie systems tend towards N-limitation, a demonstrated driver of diazotrophic abundance (Higgins et al., 2018). The secondary late-season *Planktothrix* bloom exhibited in our study has received comparatively little research in prairie systems. We noted active N-fixation verified by the presence of heterocytes during the diazotrophic bloom phase but the mechanism leading to diazotrophic collapse and replacement with *Planktothrix* remains unclear given low inorganic N (e.g., median September ammonium = ~30 µg N/L and nitrate = < LOD; Fig. 4) typically persists late into the ice-free season.

Planktothrix agardhii has been shown to thrive and form large blooms under very low to non-detectable inorganic N concentrations (e.g., Neudeck, 2018) therefore a shift in nutrient availability is unlikely to explain why *Planktothrix* forms blooms under low inorganic N conditions in autumn. It is more likely the proliferation of *Planktothrix* is due to seasonal cooling and decreased solar irradiance (Kurmayer et al., 2016). The late-season water temperatures in Buffalo Pound of just above 16 C in early September (DOY ~245) to five to eight C in early October (DOY ~270, Fig. S1), are in the ideal range for *Planktothrix* species *agardhii* and *reubescens* (Kurmayer et al., 2016; Rohrlack, 2018). As water temperatures increase above 10 C, microbial exploitation of these *Planktothrix* species has also been shown to increase (Rohrlack, 2018); therefore, we hypothesize that microbial antagonists prevent *Planktothrix* from becoming abundantly dominant in the warm summer months and may initiate *Planktothrix* population collapse (Rohrlack, 2018; Sønstebø & Rohrlack, 2011).

Interestingly, *Planktothrix* was able to amass nearly one third of the mid-summer Group B biomass in 2018 despite higher summer water temperatures (typically > 20 C). Anabaenopeptins were also present in greater amounts (e.g., anabaenopeptin B > 2000 µg/L) during the same time frame in 2018. *Planktothrix* may use these cyanopeptides as a defense mechanism in response to microbial antagonists as illustrated by Rohrlack et al. (2013), considering the warm mid-summer water temperature (> 20 C) when *Planktothrix* abundance began to build in 2018 would have been ideal for microbial growth. In 2019, *Planktothrix* was not abundant until the late season bloom, even serving as a Group C indicator, thus it is possible anabaenopeptins were not produced in

the high concentrations seen in 2018 given that cooler prevailing temperatures in September would have provided refuge from microbial attack.

Planktothrix may use cyanopeptides to displace other bloom-forming cyanobacterial species via niche construction (Kurmayer et al., 2016; Monteiro et al., 2021). For example, Sedmak et al. (2009) demonstrated that peptides including anabaenopeptin B isolated from *P. reubescens* induced lysis of *M. aeruginosa* via virus-like cyanophages and suggested that bloom conditions (e.g., high density of host cells and peptide-producing cells) likely accelerate this lytic cycle and may trigger bloom collapse. Microcystins released during the lysis of other cyanobacterial species may even act as nutrient source to *Planktothrix* (Toporowska et al., 2020). It is therefore possible the high concentrations of anabaenopeptins produced in *Planktothrix* cells in 2018 were in response to the presence of other microcystin-producing cyanobacterial species (e.g., *Dolichospermum spp.*).

In addition to their possible effects on other cyanobacterial species, anabaenopeptins may also stimulate the growth and dominance of *Planktothrix* via heterotrophic pathways. *Planktothrix* spp. are capable of phytoheterotrophy and can energize slow filament growth using in-lake carbon sources even at very low irradiance (Zotina et al., 2003). Cyanometabolites, such as anabaenopeptins, are rich in C and N and may serve as major nutrient sources to heterotrophic bacteria that occur concurrently with phytoplankton blooms (Monteiro et al., 2021; Seymour et al., 2017). These nutrient-rich peptides, as well as other complex molecules produced by cyanobacteria, are taken up and subsequently re-mineralized by heterotrophs – a pathway that could serve as an important labile nutrient source to *Planktothrix* during photoheterotrophy (Monteiro et al., 2021; Toporowska et al., 2020). The recycling of cyanomaetablites into more usable forms of C and N by hetetrophs therefore likely aids the existence of *Planktothrix* in low-light environments when energy production from photosynthesis is limited.

Our finding that chl-*a* concentrations did not capture the later *Planktothrix* bloom are consistent with the hypothesis that *Planktothrix* in Buffalo Pound are photoheterotrophic. Less light is required to energize photoheterotrophy than photosynthesis (Vonshak et al., 2000; Zotina et al., 2003); thus, likely resulting in reduced chl-*a* production late in the season when irradiance is low. However, it is also possible that commonly used methods to measure chl-*a* may not always detect *Planktothrix spp.* biomass. For example, Wentzky et al. (2019) reported this lack of association for *P. ruebescens* due to the red pigment phycoerythrin which is detected at different wavelengths (e.g., 525 and 570 nm, Fournier et al., 2021) than those commonly used to detect chl-*a* (e.g., 659, 655, and 750 nm; see methods). *Planktothrix* in Buffalo Pound was identified as *P. agardhii*, or "green" *Planktothrix*, which typically lacks phycoerythrin (Suda et al., 2002). However, morphology alone may not be sufficient to identify similar species within the same genera (Pérez-Carrascal et al. 2019). Recent work has shown *P. agardhii* and *P. reubescens* can have significant genetic overlap, including horizontal gene transfer of the phycoerythrin gene cluster between the two species thus resulting

in both red and green phenotypes (Tooming-Klunderud et al., 2013; Rohrlack, 2018). It is conceivable that *P. reubescens* existed in Buffalo Pound or, more likely, its deeper upstream reservoir previously, therefore an extremely low light adapted "red" phenotype of *P. agardhii* is a logical possibility; however algal filaments with red colouration have not been noted in raw intake water at the water treatment plant (Blair Kardash, BPWTP, pers. comm.).

Our results indicate that, under current conditions, the *Planktothrix* bloom poses an unknown t risk to human and wildlife health (Lenz et al., 2018) than the earlier *Dolichospermum* bloom given the lack of association of *Planktothrix* with toxic microcystins and the fact that anabaenopeptin toxicity is less studied than microcystin toxicity (Monteiro et al., 2021). Yet despite the correlations we have found, biomass is not indicative of toxin production so without deeper analysis (e.g., at the metagenomic level) we cannot conclude that a particular species has a causal relationship with any individual cyanobacterial metabolite. Besides, toxicogenic strains of *P. agardhii* have been widely observed elsewhere in temperate Canadian systems (e.g., in Lake Erie, Jankowiak et al., 2019) and environmental drivers may in fact mediate toxin-producing gene activity (Kurmayer et al., 2016); thus, it is possible that toxin expression by the late season *Planktothrix* bloom in Buffalo Pound may change depending on other factors not explored here (e.g., changing climatic conditions or nutrient sources). As such, continued monitoring and study of this important late season bloom is needed to establish possible toxin risk.

The largest amount of biomass during the sampling period in both years was recorded during the *Planktothrix* bloom. Given that *Planktothrix* is both filamentous and can potentially produce toxins, the ability to detect it is critical for drinking water operations. However, our results show that the most cost-effective and easy-to-use chl-*a* sensors and laboratory methods may not provide operators with reliable indication of increasing *Planktothrix* biomass as solar irradiance declines later in the year. We found the presence of *Woronichinia compacta* to be a strong indicator of the conditions in which large *Planktothrix* blooms occurred but given community stability between years, we hypothesize that a *Planktothrix* bloom is likely to predictably occur in the late summer and autumn months. Moreover, given its abundance compared to *W. compacta,* drinking water operators who routinely use microscopy are likely to find *Planktothrix* itself easier to target and identify in their weekly samples. Such information can be used to supplement chl-*a* concentrations and algal cell counts to allow for better preparation for potential water treatment challenges posed by large amounts of buoyant, filamentous biomass. However, identification of indicators may require technicians to go beyond the basic algal idenitfcation outlined in standard methods. Given the scale and urgency of the problems posed by cyanobacterial blooms, updated guidance for the idenitfcation of cyanobacterial species should therefore be a priority for regulators.

Our finding of common seasonal patterns and indicators each year suggests there is underlying stability to community structure; however, environmental

variables are likely driving the differences in magnitude and timing of blooms and their associated cyanotoxins observed in the two years. For example, succession between community groups occurred earlier in 2018 than in 2019 and the cyanobacterial community was, for the most part, *Planktothrix*-dominated after mid-July. However, in 2019, the bloom phases occurred two weeks to one month later, with the *Planktothrix* bloom only taking hold at the end of August. Moreover, N-fixation and diazotrophic abundance was also greater in 2019. These findings point to differences in nutrient availability and climatic conditions (e.g., temperature, precipitation, wind, and runoff) acting to modulate bloom formation and collapse. Future work should explore the environmental drivers of the bloom phylogeny illustrated here to better enable the prediction of these distinct bloom phases.

Our work has shown two distinct cyanobacterial bloom phases in the ice-free months, one dominated by microcystin-producing diazotrophs, the other by abundant *Planktothrix* biomass. Each present unique challenges to water treatment operators; however, biomass indicators (e.g., chl-a) and microscopically identified indicator species can be used together by managers to aid in the prediction and mitigation of bloom impacts on drinking water production. Genetic analysis of the autumn cyanobacterial community could help reconcile the taxamonic identification of *Planktothrix agardhii* in Buffalo Pound Lake with possible morphological plasticity; however, effective management relies on methods that are within-reach of water treatment managers. We also caution that although chl-a remains an important tool, it may not be ideal for assessing localized bloom risk when *Planktothrix* is a dominant bloom-forming species. For example, BPWTP attempted cessation of autumn pre-chlorination in 2021, and, despite low sensor-detected chl-a in the lake, found buoyant floc accumulating in the clarifiers within 12 hours co-occurring with positive identification of *Planktothrix* via in-house microscopy of raw intake water (Blair Kardash, BPWTP, pers. comm.).

The similarity in patterns observed over two years is certainly useful to understand this complex system but it is not certain that those two years are necessarily representative of current or future conditions in Buffalo Pound Lake. With mounting threats to water security in the Saskatchewan River Basin (Wheater & Gober, 2013), and large-scale irrigation development planned (Lake Diefenbaker Irrigation Projects, 2021) directly upstream, understanding and protection of this key drinking water resource in the face of change is increasingly critical. Climate models for the prairie region continue to point to increased future warming (Dibike et al., 2021) and there is a growing body of evidence suggesting harmful blooms and their toxins will increase in shallow, polymictic prairie lakes like Buffalo Pound (e.g., Hayes et al., 2020). The impacts of this warming may be an increasingly toxic mid-season N-fixing bloom which could exacerbate the challenges for toxin removal. The potential for increased landscape runoff from more severe precipitation events could bring further water treatment challenges related to disinfection by-products if delivery of DOM to the lake increases. Autumn irradiance will remain low regardless, thus with

23

longer ice-free seasons induced by climate warming, filamentous *Planktothrix* is likely to proliferate in deeper areas of the lake (e.g., near BPWTP intake) later into the year — as suggested by recent reports of *P. agardhii* blooms (and their toxins) persisting through the winter under ice (Wejnerowski et al., 2018). Improved understanding of the autumn *Planktothrix* bloom, its persistence, and its potential to produce toxins will be increasingly important, thus we recommend targeted study of this key bloom phase, and its potential indicators, in the future.

Acknowledgments

Open Research

The taxonomy, cyanotoxin, and nutrient data, figures and associated code used to describe the cyanobacterial community of Buffalo Pound Lake are available at the following URL: https://github.com/biogeochem/buffalopound_bloom s. **Reviewers can anonymously review at this URL; a DOI will be obtained upon paper acceptance.**

References

Ali, G., & English, C. (2019). Phytoplankton blooms in Lake Winnipeg linked to selective water-gatekeeper connectivity. *Scientific reports*, *9*(1), 1-10. https://doi.org/10.1038/s41598-019-44717-y

Binding, C. E., Greenberg, T. A., McCullough, G., Watson, S. B., & Page, E. (2018). An analysis of satellite-derived chlorophyll and algal bloom indices on Lake Winnipeg. *Journal of Great Lakes Research*, *44*(3), 436-446. https://doi.org/10.1016/j.jglr.2018.04.001

Bogard, M. J., Vogt, R. J., Hayes, N. M., & Leavitt, P. R. (2020). Unabated nitrogen pollution favors growth of toxic Cyanobacteria over Chlorophytes in

most hypereutrophic lakes. *Environmental science & technology*, *54*(6), 3219-3227. https://doi.org/10.1021/acs.est.9b06299

Buffalo Pound Water. (2020). Board of Directors Annual Report. Retrieved from: https://www.buffalopoundwtp.ca/images/content/annual-report-2020.pdf

Bunting, L., Leavitt, P. R., Simpson, G. L., Wissel, B., Laird, K. R., Cumming, B. F., ... & Engstrom, D. R. (2016). Increased variability and sudden ecosystem state change in Lake Winnipeg, Canada, caused by 20th century agriculture. *Limnology and Oceanography*, *61*(6), 2090-2107. https://doi.org/10.1002/lno.10355

Cavaliere, E., & Baulch, H. M. (2021). Winter in two phases: Long-term study of a shallow reservoir in winter. *Limnology and Oceanography*, *66*(4), 1335-1352. https://doi.org/10.1002/lno.11687

CTV News. (2015). Buffalo Pound Lake outflows increased as water issues linger. Retrieved from: https://regina.ctvnews.ca/buffalo-pound-lake-outflows-increased-as-water-issues-linger-

De Cáceres, M., Legendre, P., & Moretti, M. (2010). Improving indicator species analysis by combining groups of sites. *Oikos*, *119*(10), 1674-1684. https://doi.org/10.1111/j.1600-0706.2010.18334.x

De Cáceres, M., Jansen, F., & Dell, N. 2020 Package 'indicspecies': Relationships between species and groups of sites. https://cran.r-project.org/web/packages/indicspecies/indicspecies.pdf

Dibike, Y., Muhammad, A., Shrestha, R. R., Spence, C., Bonsal, B., de Rham, L., ... & Stadnyk, T. (2021). Application of dynamic contributing area for modelling the hydrologic response of the Assiniboine River basin to a changing climate. Journal of Great Lakes Research, 47(3), 663-676. https://doi.org/10.1016/j.jglr.2020.10.010

Dinh, Q. T., Munoz, G., Simon, D. F., Duy, S. V., Husk, B., & Sauvé, S. (2021). Stability issues of microcystins, anabaenopeptins, anatoxins, and cylindrospermopsin during short-term and long-term storage of surface water and drinking water samples. *Harmful Algae*, *101*, 101955. https://doi.org/10.1016/j.hal.2020.101955

Dufrêne, M., & Legendre, P. (1997). Species assemblages and indicator species: the need for a flexible asymmetrical approach. *Ecological monographs*, *67*(3), 345-366. https://doi.org/10.1890/0012-9615(1997)067[0345:SAAIST]2.0.CO;2

Dumanski, S., Pomeroy, J. W., & Westbrook, C. J. (2015). Hydrological regime changes in a Canadian Prairie basin. *Hydrological Processes*, *29*(18), 3893-3904. https://doi.org/10.1002/hyp.10567

Esri Canada & Natural Earth Vector. (2020). Provinces and Territoreis of Canada. ArcGIS Online via ArcGIS Pro 10.6. Redlands, CA: Environmental Systems Research Institute.

Fayad, P. B., Roy-Lachapelle, A., Duy, S. V., Prévost, M., & Sauvé, S. (2015). On-line solid-phase extraction coupled to liquid chromatography tandem mass

spectrometry for the analysis of cyanotoxins in algal blooms. *Toxicon*, *108*, 167-175. https://doi.org/10.1016/j.toxicon.2015.10.010

Findlay, D. L., & Kling, H. J. (2003). Protocols for measuring biodiversity: phytoplankton in freshwater. Winnipeg, Canada: Department of Fisheries and Oceans.

Fournier, C., Riehle, E., Dietrich, D. R., & Schleheck, D. (2021). Is Toxin-Producing Planktothrix sp. an Emerging Species in Lake Constance?. *Toxins*, *13*(9), 666. https://doi.org/10.3390/toxins13090666

Gibson, J. J., Birks, S. J., Yi, Y., Moncur, M. C., & McEachern, P. M. (2016). Stable isotope mass balance of fifty lakes in central Alberta: Assessing the role of water balance parameters in determining trophic status and lake level. *Journal of Hydrology: Regional Studies*, *6*, 13-25. https://doi.org/10.1016/j.ejrh.2016.01.034

Hayes, N. M., Haig, H. A., Simpson, G. L., & Leavitt, P. R. (2020). Effects of lake warming on the seasonal risk of toxic cyanobacteria exposure. *Limnology and Oceanography Letters*, *5*(6), 393-402. https://doi.org/10.1002/lol2.10164

Hayes, N. M., Patoine, A., Haig, H. A., Simpson, G. L., Swarbrick, V. J., Wiik, E., & Leavitt, P. R. (2019). Spatial and temporal variation in nitrogen fixation and its importance to phytoplankton in phosphorus-rich lakes. *Freshwater Biology*, *64*(2), 269-283. https://doi.org/10.1111/fwb.13214

Health Canada. (2021) Guidelines for Canadian Drinking Water Quality: Guideline Technical Document – Cyanobacterial Toxins. Retrieved from: https://www.canada.ca/en/health-canada/services/publications/healthy-living/guidelines-canadian-drinking-v

Heisler, J., Glibert, P. M., Burkholder, J. M., Anderson, D. M., Cochlan, W., Dennison, W. C., ... & Suddleson, M. (2008). Eutrophication and harmful algal blooms: a scientific consensus. *Harmful algae*, *8*(1), 3-13. https://doi.org/10.1016/j.hal.2008.08.006

Higgins, S. N., Paterson, M. J., Hecky, R. E., Schindler, D. W., Venkiteswaran, J. J., & Findlay, D. L. (2018). Biological nitrogen fixation prevents the response of a eutrophic lake to reduced loading of nitrogen: evidence from a 46-year whole-lake experiment. *Ecosystems*, *21*(6), 1088-1100. https://doi.org/10.1007/s10021-017-0204-2

Ho, J. C., Michalak, A. M., & Pahlevan, N. (2019). Widespread global increase in intense lake phytoplankton blooms since the 1980s. *Nature*, *574*(7780), 667-670. https://doi.org/10.1038/s41586-019-1648-7

Huisman, J., Codd, G. A., Paerl, H. W., Ibelings, B. W., Verspagen, J. M., & Visser, P. M. (2018). Cyanobacterial blooms. *Nature Reviews Microbiology*, *16*(8), 471-483. https://doi.org/10.1038/s41579-018-0040-1

Jalili, F.; Trigui, H.; Guerra Maldonado, J.F.; Dorner, S.; Zamyadi, A.; Shapiro, B.J.; Terrat, Y.; Fortin, N.; Sauvé, S.; Prévost, M. Can Cyanobacterial

Diversity in the Source Predict the Diversity in Sludge and the Risk of Toxin Release in a Drinking Water Treatment Plant? Toxins 2021, 13, 25. https://doi.org/10.3390/toxins13010025

Jankowiak, J., Hattenrath-Lehmann, T., Kramer, B. J., Ladds, M., & Gobler, C. J. (2019). Deciphering the effects of nitrogen, phosphorus, and temperature on cyanobacterial bloom intensification, diversity, and toxicity in western Lake Erie. *Limnology and oceanography*, *64*(3), 1347-1370. https://doi.org/10.1002/lno.11120

Kehoe, M. J., Chun, K. P., & Baulch, H. M. (2015). Who smells? Forecasting taste and odor in a drinking water reservoir. *Environmental science & technology*, *49*(18), 10984-10992. https://doi.org/10.1021/acs.est.5b00979

Kosten, S., Huszar, V. L., Bécares, E., Costa, L. S., van Donk, E., Hansson, L. A., ... & Scheffer, M. (2012). Warmer climates boost cyanobacterial dominance in shallow lakes. *Global Change Biology*, *18*(1), 118-126. https://doi.org/10.1111/j.1365-2486.2011.02488.x

Kurmayer, R., Deng, L., & Entfellner, E. (2016). Role of toxic and bioactive secondary metabolites in colonization and bloom formation by filamentous cyanobacteria Planktothrix. *Harmful algae*, *54*, 69-86. https://doi.org/10.1016/j.hal.2016.01.004

Lake Diefenbaker Irrigation Projects. (2021). Retrieved from: https://diefenbakerirrigation.ca/

Larsen, M. L., Baulch, H. M., Schiff, S. L., Simon, D. F., Sauvé, S., & Venkiteswaran, J. J. (2020). Extreme rainfall drives early onset cyanobacterial bloom. *FACETS*, *5*(1), 899-920. https://doi.org/10.1139/facets-2020-0022

Legendre, P., & Gallagher, E. D. (2001). Ecologically meaningful transformations for ordination of species data. *Oecologia*, *129*(2), 271-280. https://doi.org/10.1007/s004420100716

Lenz, K. A., Miller, T. R., & Ma, H. (2019). Anabaenopeptins and cyanopeptolins induce systemic toxicity effects in a model organism the nematode Caenorhabditis elegans. Chemosphere, 214, 60-69. https://doi.org/10.1016/j.chemosphere.2018.09.076

Loewen, C. J., Vinebrooke, R. D., & Zurawell, R. W. (2021). Quantifying seasonal succession of phytoplankton trait-environment associations in human-altered landscapes. *Limnology and Oceanography*, *66*(4), 1409-1423. https://doi.org/10.1002/lno.11694

Monteiro, P. R., do Amaral, S. C., Siqueira, A. S., Xavier, L. P., & Santos, A. V. (2021). Anabaenopeptins: What We Know So Far. *Toxins*, *13*(8), 522. https://doi.org/10.3390/toxins13080522

Moradinejad, S., Glover, C. M., Mailly, J., Seighalani, T. Z., Peldszus, S., Barbeau, B., ... & Zamyadi, A. (2019). Using advanced spectroscopy and organic matter characterization to evaluate the impact of oxidation on cyanobacteria. Toxins, 11(5), 278.https://doi.org/10.3390/toxins11050278

Moradinejad, S., Trigui, H., Guerra Maldonado, J. F., Shapiro, J., Terrat, Y., Zamyadi, A., ... & Prévost, M. (2020). Diversity Assessment of Toxic Cyanobacterial Blooms during Oxidation. Toxins, 12(11), 728. https://doi.org/10.3390/toxins12110728

Munoz, G., Duy, S. V., Roy-Lachapelle, A., Husk, B., & Sauvé, S. (2017). Analysis of individual and total microcystins in surface water by on-line pre-concentration and desalting coupled to liquid chromatography tandem mass spectrometry. *Journal of Chromatography A*, *1516*, 9-20. https://doi.org/10.1016/j.chroma.2017.07.096

Natural Resources Canada. (2019). CanVec. Available from: https://maps.canada.ca/czs/index-en.html

Neudeck, M. J. (2018). Tolerance of Planktothrix agardhii to nitrogen depletion, (Master's thesis). Retrieved from OhioLINK Electronic Theses and Dissertations Center. (http://rave.ohiolink.edu/etdc/view?acc_num=bgsu1522329471601801). Bowling Green, OH: Bowling Green State University.

Oksanen, J., Blanchet, F. G., Friendly, M., Kindt, R., Legendre, P., McGlinn, D., ... & Wagner H. (2020). Package vegan. Retrieved from: https://cran.r-project.org/web/packages/vegan/vegan.pdf

Orihel, D. M., Bird, D. F., Brylinsky, M., Chen, H., Donald, D. B., Huang, D. Y., ... & Vinebrooke, R. D. (2012). High microcystin concentrations occur only at low nitrogen-to-phosphorus ratios in nutrient-rich Canadian lakes. Canadian Journal of Fisheries and Aquatic Sciences, 69(9), 1457-1462. https://doi.org/10.1139/f2012-088

Orihel, D. M., Schindler, D. W., Ballard, N. C., Graham, M. D., O'Connell, D. W., Wilson, L. R., & Vinebrooke, R. D. (2015). The "nutrient pump:" Iron-poor sediments fuel low nitrogen-to-phosphorus ratios and cyanobacterial blooms in polymictic lakes. *Limnology and Oceanography*, *60*(3), 856-871. https://doi.org/10.1002/lno.10076

Paerl, H. W., & Huisman, J. (2009). Climate change: a catalyst for global expansion of harmful cyanobacterial blooms. *Environmental microbiology reports*, *1*(1), 27-37. https://doi.org/10.1111/j.1758-2229.2008.00004.x

Pérez-Carrascal, O. M., Terrat, Y., Giani, A., Fortin, N., Greer, C. W., Tromas, N., & Shapiro, B. J. (2019). Coherence of Microcystis species revealed through population genomics. The ISME journal, 13(12), 2887-2900. https://doi.org/10.1038/s41396-019-0481-1

Persaud, A. D., Paterson, A. M., Dillon, P. J., Winter, J. G., Palmer, M., & Somers, K. M. (2015). Forecasting cyanobacteria dominance in Canadian temperate lakes. *Journal of environmental management*, *151*, 343-352. https://doi.org/10.1016/j.jenvman.2015.01.009

Public Health Agency of Canada. (2013). Guidelines for Canadian Drinking Water Quality: Guideline Technical Document – Trihalomethanes. Retrieved from:

https://www.canada.ca/en/health-canada/services/publications/healthy-living/guidelines-canadian-drinking-v

R Core Team. (2021). R: A language and environment for statistical computing. Vienna, Austria: R Foundation for Statistical Computing.

Rohrlack, T. (2018). Low temperatures can promote cyanobacterial bloom formation by providing refuge from microbial antagonists. *AIMS microbiology*, *4*(2), 304. doi: 10.3934/microbiol.2018.2.304

Rohrlack, T., Christiansen, G., & Kurmayer, R. (2013). Putative antiparasite defensive system involving ribosomal and nonribosomal oligopeptides in cyanobacteria of the genus Planktothrix. *Applied and environmental microbiology*, *79*(8), 2642-2647. https://doi.org/10.1128/AEM.03499-12

Roy-Lachapelle, A., Duy, S. V., Munoz, G., Dinh, Q. T., Bahl, E., Simon, D. F., & Sauvé, S. (2019). Analysis of multiclass cyanotoxins (microcystins, anabaenopeptins, cylindrospermopsin and anatoxins) in lake waters using on-line SPE liquid chromatography high-resolution Orbitrap mass spectrometry. *Analytical Methods*, *11*(41), 5289-5300. https://doi.org /10.1039/C9AY01132C

Schindler, D. W., & Donahue, W. F. (2006). An impending water crisis in Canada's western prairie provinces. *Proceedings of the National Academy of Sciences*, *103*(19), 7210-7216. https://doi.org/10.1073/pnas.0601568103

Schindler, D. W., Hecky, R. E., & McCullough, G. K. (2012). The rapid eutrophication of Lake Winnipeg: Greening under global change. *Journal of Great Lakes Research*, *38*, 6-13. https://doi.org/10.1073/pnas.0601568103

Sedmak, B., Carmeli, S., Pompe-Novak, M., Tušek-Žnidarič, M., Grach-Pogrebinsky, O., Eleršek, T., ... & Frangež, R. (2009). Cyanobacterial cytoskeleton immunostaining: the detection of cyanobacterial cell lysis induced by planktopeptin BL1125. Journal of plankton research, 31(11), 1321-1330.https://doi.org/10.1093/plankt/fbp076

Seymour, J. R., Amin, S. A., Raina, J. B., & Stocker, R. (2017). Zooming in on the phycosphere: the ecological interface for phytoplankton–bacteria relationships. *Nature microbiology*, *2*(7), 1-12. https://doi.org/10.1038/nmicrobiol.2017.65

Sønstebø, J. H., & Rohrlack, T. (2011). Possible implications of chytrid parasitism for population subdivision in freshwater cyanobacteria of the genus Planktothrix. *Applied and environmental microbiology*, *77*(4), 1344-1351. https://doi.org/10.1128/AEM.02153-10

Species at Risk Public Registry. (2011). Bigmouth Buffalo Saskatchewan – Nelson River populations. Retrieved from: https://wildlife-species.canada.ca/species-risk-registry/species/speciesI

Suda, S., Watanabe, M. M., Otsuka, S., Mahakahant, A., Yongmanitchai, W., Nopartnaraporn, N., ... & Day, J. G. (2002). Taxonomic revision of water-bloom-forming species of oscillatorioid cyanobacteria. International journal of systematic and evolutionary microbiology, 52(5), 1577-1595. https://doi.org/10.1099/00207713-52-5-1577

Taranu, Z. E., Gregory-Eaves, I., Leavitt, P. R., Bunting, L., Buchaca, T., Catalan, J., ... & Vinebrooke, R. D. (2015). Acceleration of cyanobacterial dominance in north temperate-subarctic lakes during the Anthropocene. *Ecology letters*, *18*(4), 375-384. https://doi.org/10.1111/ele.12420

Terry, J. (2020). Water quality modelling of Buffalo Pound Lake, (Doctoral dissertation). Retrieved from HARVEST. (http://hdl.handle.net/10388/12787). Saskatoon, Canada: University of Saskatchewan.

Terry, J. A., Sadeghian, A., & Lindenschmidt, K. E. (2017). Modelling dissolved oxygen/sediment oxygen demand under ice in a shallow eutrophic prairie reservoir. *Water*, *9*(2), 131. https://doi.org/10.3390/w9020131

Tooming-Klunderud, A., Sogge, H., Rounge, T. B., Nederbragt, A. J., Lagesen, K., Glöckner, G., ... & Jakobsen, K. S. (2013). From green to red: Horizontal gene transfer of the phycoerythrin gene cluster between Planktothrix strains. *Applied and environmental microbiology*, *79*(21), 6803-6812. https://doi.org/10.1128/AEM.01455-13

Toporowska, M., Mazur-Marzec, H., & Pawlik-Skowrońska, B. (2020). The effects of cyanobacterial bloom extracts on the biomass, Chl-a, MC and other oligopeptides contents in a natural Planktothrix agardhii population. *International journal of environmental research and public health*, *17*(8), 2881. https://doi.org/10.3390/ijerph17082881

Tse, T. J., Doig, L. E., Tang, S., Zhang, X., Sun, W., Wiseman, S. B., ... & Jones, P. D. (2018). Combining high-throughput sequencing of seda DNA and traditional paleolimnological techniques to infer historical trends in cyanobacterial communities. *Environmental science & technology*, *52*(12), 6842-6853. https://doi.org/10.1021/acs.est.7b06386

Visser, P. M., Verspagen, J. M., Sandrini, G., Stal, L. J., Matthijs, H. C., Davis, T. W., ... & Huisman, J. (2016). How rising CO2 and global warming may stimulate harmful cyanobacterial blooms. *Harmful Algae*, *54*, 145-159. https://doi.org/10.1016/j.hal.2015.12.006

Vogt, R. J., Sharma, S., & Leavitt, P. R. (2018). Direct and interactive effects of climate, meteorology, river hydrology, and lake characteristics on water quality in productive lakes of the Canadian Prairies. *Canadian Journal of Fisheries and Aquatic Sciences*, *75*(1), 47-59. https://doi.org/10.1139/cjfas-2016-0520

Vollenweider, R. A. (1968). Scientific fundamentals of the eutrophication of lakes and flowing waters, with particular reference to nitrogen and phosphorus as factors in eutrophication. (Technical Report DAS/CS1/68.27. Vol. 3). Paris, France: Organisation for Economic Co-Operation and Development.

Vonshak, A., Cheung, S. M., & Chen, F. (2000). Mixotrophic growth modifies the response of Spirulina (Arthrospira) platensis (Cyanobacteria) cells to light. *Journal of Phycology*, *36*(4), 675-679. https://doi.org/10.1046/j.1529-8817.2000.99198.x

Water Security Agency. (2021). Buffalo Pound Lake. Retrieved from: https://www.wsask.ca/lakes-rivers/dams-reservoirs/major-dams-and-reservoirs/buffalo-pound-lake/

Wejnerowski, Ł., Rzymski, P., Kokociński, M., & Meriluoto, J. (2018). The structure and toxicity of winter cyanobacterial bloom in a eutrophic lake of the temperate zone. *Ecotoxicology*, *27*(6), 752-760. https://doi.org/10.1007/s10646-018-1957-x

Wentzky, V. C., Frassl, M. A., Rinke, K., & Boehrer, B. (2019). Met-alimnetic oxygen minimum and the presence of Planktothrix rubescens in a low-nutrient drinking water reservoir. *Water research*, *148*, 208-218. https://doi.org/10.1016/j.watres.2018.10.047

Wheater, H., & Gober, P. (2013). Water security in the Canadian Prairies: science and management challenges. *Philosophical Transactions of the Royal Society A: Mathematical, Physical and Engineering Sciences*, *371*(2002), 20120409. https://doi.org/10.1098/rsta.2012.0409

Wintermans, J. F. G. M., & De Mots, A. S. (1965). Spectrophotometric characteristics of chlorophylls a and b and their phenophytins in ethanol. *Biochimica et Biophysica Acta (BBA)-Biophysics including Photosynthesis*, *109*(2), 448-453. https://doi.org/10.1016/0926-6585(65)90170-6

World Health Organization. (2011). Managing cyanobacteria in drinking water supplies: information for regulators and water suppliers (WHO/FWC/WSH/15.03). Retrieved from: https://www.who.int/water_sanitation_health/dwq/cyanobacteria_in_drinking-water.pdf

World Health Organization. (2020). Cyanobacterial toxins: microcystins. Background document for development of WHO Guidelines for drinking-water quality and Guidelines for safe recreational water environments (WHO/HEP/ECH/WSH/2020.6). Retrieved from: https://apps.who.int/iris/bitstream/handle/10665/338066/HEP-ECH-WSH-2020.6-eng.pdf

Zamyadi, A., Choo, F., Newcombe, G., Stuetz, R., & Henderson, R. K. (2016). A review of monitoring technologies for real-time management of cyanobacteria: Recent advances and future direction. *Trends in Analytical Chemistry*, 85, 83-96. https://doi.org/10.1016/j.trac.2016.06.023

Zamyadi, A., Romanis, C., Mills, T., Neilan, B., Choo, F., Coral, L. A., ... & Henderson, R. K. (2019). Diagnosing water treatment critical control points for cyanobacterial removal: Exploring benefits of combined microscopy, next-generation sequencing, and cell integrity methods. *Water Research*, 152, 96-105., https://doi.org/10.1016/j.watres.2019.01.002

Zamyadi, A., Glover, C. M., Yasir, A., Stuetz, R., Newcombe, G., Crosbie, N. D., ... & Henderson, R. (2021). Toxic cyanobacteria in water supply systems: data analysis to map global challenges and demonstrate the benefits of multi-barrier treatment approaches. *H$_2$Open Journal*, *4*(1), 47-62. https://doi.org/10.2166/h2oj.2021.067

Zotina, T., Köster, O., & Jüttner, F. (2003). Photoheterotrophy and light-dependent uptake of organic and organic nitrogenous compounds by Planktothrix rubescens under low irradiance. *Freshwater Biology*, *48*(10), 1859-1872. https://doi.org/10.1046/j.1365-2427.2003.01134.x